

SCIENTIFIC REPORTS



OPEN

Optical and THz investigations of mid-IR materials exposed to alpha particle irradiation

Dan Sporea¹, Laura Mihai¹, Adelina Sporea¹ & Ion Vâță²

Received: 29 September 2016

Accepted: 01 December 2016

Published: 09 January 2017

The paper is the first comprehensive study on alpha particle irradiation effects on four mid-IR materials: CaF_2 , BaF_2 , Al_2O_3 (sapphire) and ZnSe . The measurements of the optical spectral transmittance, spectral diffuse reflectance, radioluminescent emission, terahertz (THz) spectral response, transmittance, absorbance, refractive index, real and imaginary parts of the dielectric constant and THz imaging are used as complementary investigations to evaluate these effects. The simulations were run to estimate: (i) the penetration depth, (ii) the scattering of alpha particle beam, (iii) the amount of material affected by this interaction, and (iv) the number of vacancies produced by the radiation exposure for each type of material. The simulation results are compared to the off-line measurement outcomes. The delay and spectral composition change of the reflected THz signal highlight the modification induced in the tested materials by the irradiation process.

Devices and equipments included as space missions constituents are subjected to energetic radiation fields such as^{1–4}: solar flare, trapped protons, trapped electrons, galactic cosmic ray – GCR (protons, alpha particles, heavy ions), radiation which might affect their normal operation. Radiation effects in materials and components are extensively considered in the last 10 years as the incidents associated with their destruction/degradation are more and more complex and expensive to circumvent during a mission, affecting normal operation, inducing components and instruments malfunction or producing major interferences in sensing systems. Designing special systems for space borne applications became an issue because of higher associated costs. For this reasons, the use of commercial off-the-shelf components (COTS), tested for their radiation hardness is nowadays a solution of choice, but this approach implies extensive testing for space operation qualification¹.

Early research done by Capasso *et al.* some twenty years ago focused on new semiconductor coherent sources operating in the mid and far IR spectral range, the quantum cascade lasers – QCLs, opened new opportunities for spectroscopy at these wavelengths⁵. Such developments facilitated the spread of applications related to astronomy, astrophysics, astrochemistry, space missions^{6,7}. High resolution spectroscopy of molecules rotation spectra is performed by SOFIA (Stratospheric Observatory for Infrared Astronomy) using heterodyne based on a QCL⁸. Other applications of QCLs for gas trace detection in planetary missions were planned⁹. The CubSat and ESA In-Orbit Demonstration unit were designed to accommodate a Laser Heterodyne Radiometer (LHR) using a QCL-based local oscillator¹⁰.

In the context implying the replacement of FTIR instrumentation designed for space missions by QCL-based equipments operating in the mid-IR, the core components involved into such setups (emitters, detectors, optical parts) have to be tested under irradiation environments.

Reports exist on the effects of various ionizing radiations on optical materials, such as:

- (i) radiation induced absorption–RIA:
 - observed over 200–800 nm for electron beam irradiated SiO_2 at room temperature and heated¹¹;
 - in BaF_2 cylindrical crystals, subjected to gamma radiation (⁶⁰Co and ¹³⁷Cs sources)¹², or irradiated with various heavy ions¹³, having optical transmission measured in the 200–800 nm spectral range;
 - over the 300 nm–850 nm spectral interval, in CaF_2 crystals exposed to thermal and fast neutron flux¹⁴ or gamma-rays¹⁵;
 - investigated in the visible-near IR (200 nm to 900 nm), in low OH content KUVI-S and high OH content KU-1 quartz glasses, and sapphire as they were subjected to electron beam, neutron, gamma-rays^{16–20};
 - measured by FTIR in the IR (1600 cm^{-1} – 4000 cm^{-1}) for neutron irradiated sapphire²¹.

¹National Institute for Laser, Plasma and Radiation Physics, Center for Advanced Laser Technologies, Magurele, RO-077125, Romania. ²“Horia Hulubei” National Institute of Physics and Nuclear Engineering, RO-077125, Magurele, Romania. Correspondence and requests for materials should be addressed to D.S. (email: dan.sporea@inflpr.ro)

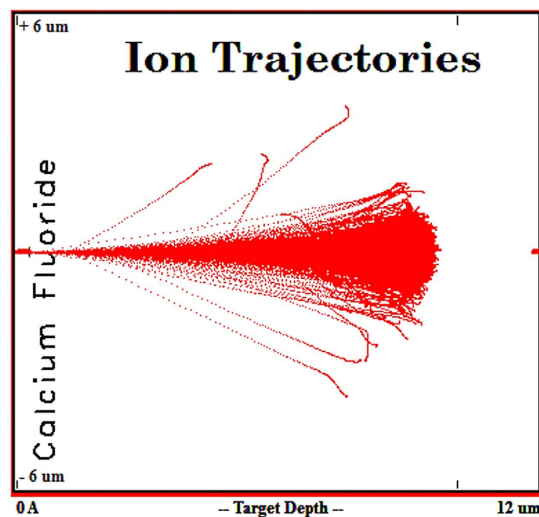


Figure 1. Result of the penetration depth simulation and scattering pattern of alpha particles in CaF_2 .

(ii) radiation induced luminescence – RIL:

- signal in SiO_2 , KU-1 glass or sapphire under electron beam, gamma-ray, neutron proton or heavy ion irradiation^{11,16,17,22–24};
- appearing in BaF_2 crystals during gamma¹² or X-ray irradiation²⁵;
- present in CaF_2 crystals where they are exposed to X-rays²⁶;
- emission in ZnSe under X-ray excitation²⁷.

In the last 15 years, THz investigations of various materials gained momentum, as new techniques started to be used for dielectric materials identification/characterization in the far IR, through the evaluation of the dielectric constant and loss tangent by time-domain terahertz spectroscopy, which make possible the measurement of both the amplitude and phase of the detected signal, or by estimating the absorption coefficients and the refractive indices of various glasses and ceramics^{28–36}.

More recently, the investigations of some active and passive optical components subjected to ionizing radiation were performed to evaluate their radiation resistivity^{37–39}.

In this paper, we report the alpha particle irradiation induced changes in four mid-IR window materials (CaF_2 , BaF_2 , Zn Se, sapphire), for their possible use in spaceborne applications. For **the first time**, the irradiation-induced characteristics are assessed by a multidisciplinary approach through optical investigations: UV to far-IR optical spectroscopy, radioluminescence measurements, THz spectroscopy and imaging.

Results

“Supplementary materials” contains information on: (i) additional results (section “Additional results”); (ii) the materials tested under this research and their specific characteristics of interest for this demarche (section “Investigated samples”); (iii) the irradiation conditions (section “Alpha particle irradiation and simulations”); (iv) the laboratory setups used for the evaluation of irradiated sample (sections “Optical investigations”, “THz spectral investigations THz imaging”). Figures and Tables to be found in this part of the work are cited in the main text accompanied by the suffix “Supplementary”.

The simulation result referring to the penetration depth and scattering of alpha particles in CaF_2 is shown in Fig. 1. The simulations for BaF_2 , Al_2O_3 and ZnSe are given in Supplementary Fig. 1, under “Additional results”. The simulations were done for beam charge of 100 000 alpha particles.

The penetration depths and the optical material mass affected by the exposure to alpha particles, as calculated according to equations Supplementary 1 and Supplementary 2, are depicted for comparison in Supplementary Fig. 2. The diagrams indicate that, on the first part of their trajectory, the particle path is quite straight as the particle energy is high, while, as particle interact with electrons, their energy diminish below the ionization threshold and it loses the velocity and produces nucleus displacements, which in turn contribute to material local density change⁴⁰.

The material is described by the chemical bonds, density and molar mass that influences the probability of collisions of alpha particle with sample lattice [Supplementary 1–5], hence determining the number of produced vacancies (Supplementary Fig. 3). In the graphs, the number of collisions is plotted as a function of penetration depth.

The Rutherford backscattering spectrometry (RBS) measurements and the corresponding simulations were run in order to: (i) check samples’ compositions, (ii) identify impurities, (iii) estimate the charge deployed during the irradiation for the calculation of the total dose. The results of our experimental findings and simulations are compared in Supplementary Fig. 4.

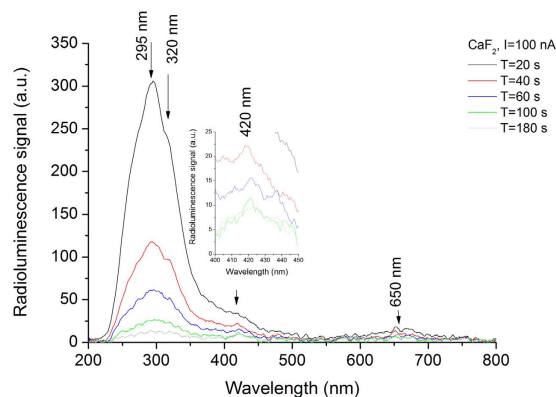


Figure 2. Radioluminescence detected spectrum under alpha particle irradiation of CaF_2 .

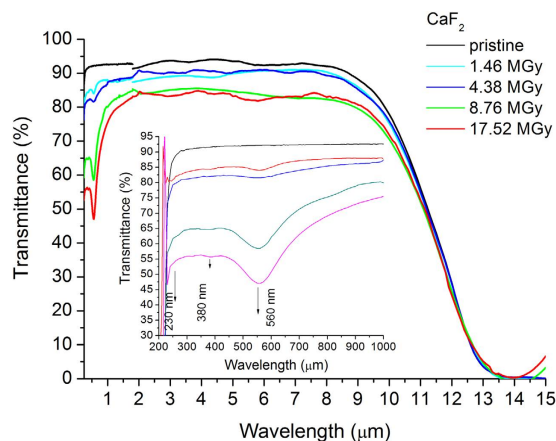


Figure 3. Spectral optical transmittance before and after alpha irradiation of CaF_2 .

By on-line measurements we monitor the radioluminescence signal generated during the irradiation by alpha particles for the four mid-IR optical materials (Fig. 2 and Supplementary Fig. 5). In each case, the beam current is specified and the detected radioluminescence peaks are identified.

Alpha particles incident on the optical windows materials produce color change as well as small craters or cracks, implying the degradation of the surface quality (Supplementary Fig. 6). This irradiation induced color modification is highlighted in Fig. 3 and Supplementary Fig. 7, as proved by the variation of the optical transmission. The details regarding the spectral absorbance are given in Supplementary Fig. 8 for easier identification of absorption peaks. The spectral diffused reflectance of the samples in the visible and near-IR spectral range is shown in Supplementary Fig. 9. The dose received by each sample by the subsequent irradiation sessions and the total dose are calculated according to Supplementary 1 – Supplementary 3 equations, in the “*Supplementary materials*” part of the paper.

One of the original points of our investigation is the study of the changes in the THz characteristics of the mid-IR materials, as induced by alpha particle irradiation. These modifications (i.e. density modifications) can be conveniently located if the THz pulse propagation is studied. THz techniques were used to evaluate crystallinity of the materials^{41,42}. The optical delay of the THz transmitted signal for pristine and irradiated CaF_2 samples is given in Fig. 4, while the optical delay of the THz reflected signal for pristine and irradiated BaF_2 , sapphire and ZnSe samples is given in Supplementary Fig. 10.

The THz signal, as obtained in the frequency domain, for the tested samples prior and after the irradiation is represented in Supplementary Fig. 11. The THz spectroscopy was proposed for the measurements of optical characteristics (refractive index, absorbance)^{43,44} and real/imaginary part of the dielectric constant^{44,45} of various materials. The results of our investigation for the mid-IR windows, as they are affected by the irradiation, are depicted in Supplementary Figs 12–15.

To further illustrate the use of THz methods in investigating the effects of alpha particle irradiation on mid-IR materials we provide some examples of THz imaging studies for pristine and irradiated CaF_2 , BaF_2 , Al_2O_3 and ZnSe samples. The variation of the THz reflected signal as a function of THz frequency for the pristine and exposed windows, as found by the frequency domain analysis mode, is shown in Fig. 5 and Supplementary Fig. 16. The images illustrate the variation along the x axis (B-scan). For the detection geometry of the reflected signal, please refer to “*THz spectral investigations THz imaging*” section of the *Supplementary materials*. The images

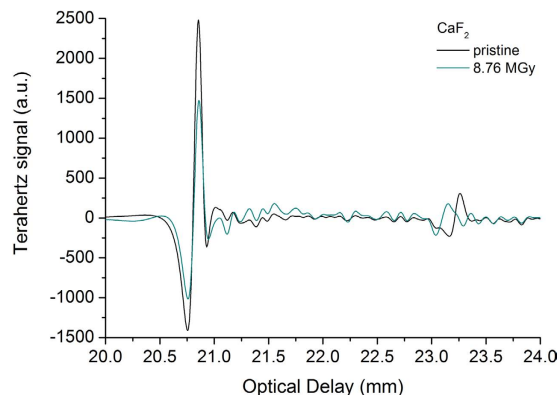


Figure 4. Delay of the transmitted THz pulse as induced by alpha particle irradiation for the case of CaF_2 .

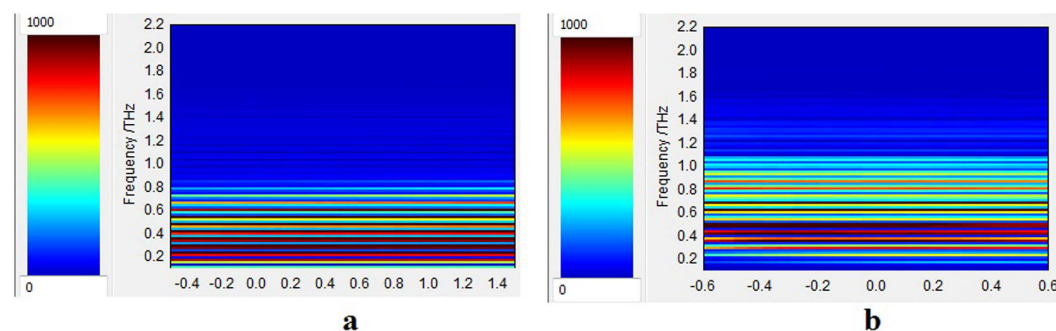


Figure 5. THz reflectance 2D image along the x axis as function of THz frequency (B-scan) using the frequency domain analysis mode for CaF_2 sample: (a) pristine window; (b) window exposed up to the dose of 8.76 MGy.

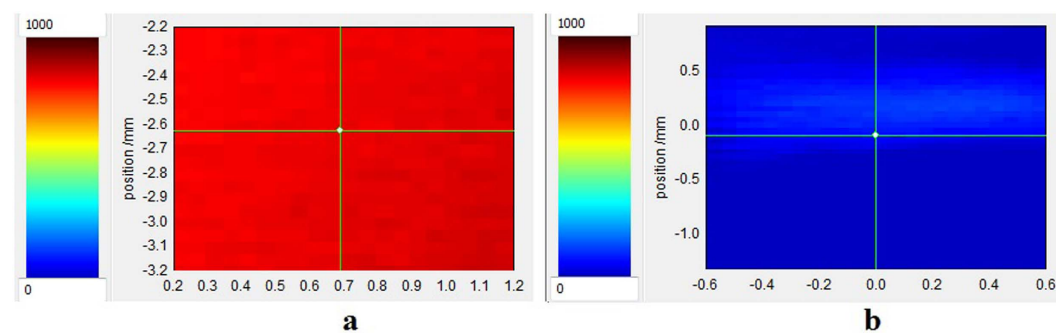


Figure 6. THz cross section in the xy plane (C-scan) using the frequency domain analysis mode for CaF_2 sample: (a) pristine window; (b) window exposed up to the dose of 4.38 MGy.

depicted in Fig. 5 and Supplementary Fig. 16 correspond to the variation of the THz signal with frequency, as represented in Supplementary Fig. 11.

The examples of xy cross sections (C-scan) through the tested samples, as generated by THz reflectance imaging before and after the irradiation, are given in Fig. 6 and Supplementary Fig. 17. Figure 6 illustrates the irradiation induced change detected under THz radiation in the CaF_2 sample over an area having no structural defects. Similar data are provided for Al_2O_3 (Supplementary Fig. 17c and d) and ZnSe (Supplementary Fig. 17e and f). In Supplementary Fig. 17a and b, the THz image of a defect localized in the BaF_2 sample is shown before and after the exposure.

The detection of the defect through THz signal reflection, as represented in the frequency domain analysis mode, can be seen very well in Supplementary Fig. 18. This information corresponds to the results presented in Supplementary Fig. 17a and b.

The similar results to the optical delay signal (Fig. 4 and Supplementary Fig. 10), represented as 2D images picked up along the Ox axis and using the time domain analysis, are shown for pristine and irradiated windows in Supplementary Fig. 19.

Discussions

From the simulations run it can be noticed that the alpha particles scatter pattern and the penetration depth (Fig. 1 and Supplementary Fig. 1) are dependent on the sample material (i.e. density, molar mass). The collision events which might produce vacancies occur at specific depths in CaF₂, Al₂O₃ or ZnSe and they spread over the entire interaction length in BaF₂ (Supplementary Fig. 3).

The behavior of the tested samples under irradiation can be influenced by some impurities. Within this context we performed RBS investigations (Supplementary Fig. 4). No impurities were detected in our measurements having the sensitivity of about 1%.

As for CaF₂, the main radioluminescence peak is observed in the UV range (Fig. 2) with components at $\lambda = 295$ nm, 320 nm and 420 nm^{26,46} and a much smaller component is detected in visible ($\lambda = 650$ nm), as it was found in the earlier published reports.

Under alpha particle exposure, BaF₂ exhibits a broad band emission from 250 nm to 750 nm (Supplementary Fig. 5a), where some peaks or spectral bands previously reported in the literature can be identified^{25,47}.

The radioluminescence from irradiated sapphire presents several peaks in UV ($\lambda = 280$ nm²⁴, 325 nm¹⁷, 420 nm^{17,18,22–24}), one major in the near-IR ($\lambda = 697$ nm^{17,18,24}) and some smaller peaks in the same region²⁴. In the case of ZnSe, the emitted spectra are present for $\lambda = 473$ nm²⁷. These peaks for sapphire and ZnSe were identified also in our study (Supplementary Fig. 5b and c).

Regarding the radiation induced optical attenuation we have noticed that:

- CaF₂ decreases its optical transmission (Fig. 3) from 350 nm to 11 μ m with a significant deep in UV-visible (up to 1 μ m);
- BaF₂ transmission (Supplementary Fig. 7a) decreases in the UV (below 500 nm) and mid-IR ranges;
- sapphire is almost not affected by the exposure (Supplementary Fig. 7b), excepting some small attenuation peaks in the near-IR (0.9 μ m–1 μ m) and the region below 300 nm;
- ZnSe transmission (Supplementary Fig. 7c) is diminished over the entire operating range (530 nm–19 μ m);

The absorption peaks related to the radiation effects in the studied materials were identified as follows:

- in CaF₂ (Supplementary Fig. 8a) at $\lambda = 379$ nm¹⁴ and 550 nm^{13,14};
- in BaF₂ (Supplementary Fig. 8b) at $\lambda = 220$ nm, 240 nm, 750 nm¹³;
- in sapphire (Supplementary Fig. 8c) at $\lambda = 220$ nm^{18,22,29}, 257 nm^{18–20,22}, 320 nm¹⁸.

Three of the tested samples (CaF₂, BaF₂, Al₂O₃) are purchased from the same manufacturer, while the ZnSe sample was acquired from another provider. As the materials are exposed to incident particles their diffused reflectance increases (Supplementary Fig. 9), supposedly as function of their mean harness (Supplementary Table 1). The diffused reflectance increase can be attributed to the surface defects (small craters/cracks) produced by the irradiation (Supplementary Fig. 6).

As the samples are subjected to alpha particle bombardment, their local properties changes were detected as a delay present in the propagation of the THz investigation pulse (Fig. 4 and Supplementary Fig. 10). Within some limits, 27.3×10^6 Gy for BaF₂, 8.67×10^6 Gy for CaF₂, alpha particle irradiation produces a change of the THz frequency signal, accompanied by a shift of the maximum towards higher frequencies (Supplementary Fig. 11a and b), while in the case of Al₂O₃ and ZnSe the THz frequency spectrum does not change and only a decrease of the amplitude can be noticed (Supplementary Fig. 11c and d). At higher total doses for CaF₂ and BaF₂ the frequency shift saturates.

Some modifications of the THz spectral refractive index upon irradiation occur for the sapphire and CaF₂ samples, while ZnSe and BaF₂ refractive index variation is smaller (Supplementary Fig. 12). The THz absorbance of CaF₂, BaF₂ seems not to be affected by the irradiation (Supplementary Fig. 13a and b), and some changes being observed for Al₂O₃ and ZnSe (Supplementary Fig. 13c and d).

The exposure to alpha particles produces a variation of the real part of dielectric constant in the case of all tested samples, while the imaginary part remains almost unchanged (Supplementary Figs 14 and 15).

The capability to monitor the irradiation induced changes by THz spectroscopy is provided by 3D mapping of these effects in the irradiated volume using different cross sections, as it is demonstrated through THz reflectance measurements (Figs 5 and 6, Supplementary Fig. 16 and Supplementary Fig. 17). The THz imaging can be used to localize material defects or anisotropic points (Supplementary Fig. 18). Additional interpretations can be derived from images obtained by time domain analysis (Supplementary Fig. 19).

After the irradiation the CaF₂ and BaF₂ samples became very brittle, as that they presented cracks or even at the end were broken into several pieces. This outcome can be attributed to the lower thermal conductivity of CaF₂ and BaF₂, as the irradiations took place in vacuum, hence poorer heat dissipation occurred in these samples producing local thermal stress.

Conclusions

We performed our study by combining various techniques in order to assess for the *first time* the changes induced in mid-IR optical materials by alpha particle irradiation. Our investigations bring several novelties to the field of material research operating in harsh environments (i.e. ionizing radiation):

1. We evaluate, as a premiere, the modifications produced by alpha particles in IR optical windows as it concerns: (i) the optical transmission over their entire spectral operating range of these materials (Fig. 3 and Supplementary Fig. 7 and Supplementary Fig. 8); (ii) the degradation of their surface roughness post

- irradiation (spectral diffusion reflectance measurements, Supplementary Fig. 9); (iii) the generated radioluminescence signal (Fig. 2 and Supplementary Fig. 5).
- We provide information on the interaction between the target material and the alpha particle beam, supported by the simulations run in relation to the penetration depth, the particle scattering inside the sample and the number of generated vacancies which might be responsible for the optical transmission degradation (Fig. 1, Supplementary Fig. 1, Supplementary Fig. 3).
 - We offer data, not available up today, on the THz refractive index, absorbance, real and imaginary parts of the dielectric constant for four mid-IR materials prior and post exposure to alpha particles (Supplementary Figs 11–14).
 - For the first time we highlight the change of these materials THz spectra, as they are subjected to irradiation (Fig. 5, Supplementary Fig. 11 and Supplementary Fig. 16).
 - The effect of the irradiation on mid-IR materials THz performances are also exemplified by the modification THz pulse delay (Fig. 4 and Supplementary Fig. 10).
 - We propose THz imaging as a mean to “visualize” the irradiation produced changes in the volume of the irradiated material, along different axes (Figs 5 and 6, Supplementary Figs 16–19).

The results of this research, constituted into an extensive database, are of interest for researchers involved in: (i) material science studies, (ii) investigation of ionizing radiation impact on optical materials, (iii) applications of THz technology, (iv) the study of scintillating materials, (v) the design of equipments to operate in harsh environments (i.e. spaceborne instrumentation).

Materials and Methods

The mid-IR optical windows tested under this investigation were provided by Skight Optics Co., Ltd., China (CaF₂, BaF₂, Al₂O₃) and Edmund Optics Ltd. (ZnSe). General characteristics of the studied materials are published in literature [Supplementary 1–5]. Specific parameters of the samples (dimensions and operating spectral range) are indicated in Supplementary Table 1 (“Supplementary materials”, section “Investigated samples”).

Irradiation conditions are described “Supplementary materials”, under section “Alpha particle irradiation and simulations”.

The irradiations were run in several subsequent steps, and, before and after each irradiation, their characteristics were measured in the optical and THz spectral range. For details concerning the setups use in laboratory (off-line) optical and THz investigations refer to “Supplementary materials”, sections “Optical investigations” and “THz spectral investigations THz imaging”.

References

- European Cooperation for Space Standardization (ECSS), *Space engineering: Space environment*, (ECSS-E-10-04A, Noordwijk http://www.spacewx.com/Docs/ECSS-E-ST-10-04C_15Nov2008.pdf) (2000).
- Barth, J. L., Dyer, C. S. & Stassinopoulos, E. G. Space, atmospheric, and terrestrial radiation environments. *IEEE Trans. Nucl. Sci.* **50**, 466–482 (2003).
- Bourdarie, S. & Xapsos, M. The near-earth space radiation environment. *IEEE Trans. Nucl. Sci.* **55**, 1810–1832 (2008).
- Vadawale, S. V., Goswami, J. N., Dachev, T. P., Tomov, B. T. & Girish, V. Radiation Environment in Earth-Moon Space: Results from Radom Experiment Onboard CHANDRAYAAN-1. *Advances in Geosciences, Planetary Science*, **25** Ed. Bhardwaj, A. (World Scientific, 2011).
- Faist, J. *et al.* Quantum Cascade Laser. *Science* **264**(5158), 553–556 (1994).
- Brumfield, B. E. *High-resolution spectroscopic studies of C₆₀ and C₆H₆: molecules of fundamental spectroscopic and astrochemical importance*, Preliminary examination, November 2007.
- Tasinato, N. *Infrared spectroscopy of atmospheric and astrophysical relevant molecules: spectral analysis, line parameter retrievals and study of collisional decay processes*, Doctoral Thesis, Università Ca' Foscari Venezia (2009).
- Hübers H.-W. *et al.* Liquid-cryogen free front-end for a 2.5-THz heterodyne receiver, *Proceedings of 22nd International Symposium on Space Terahertz Technology*, Tucson, (2011).
- Wilson, C. F. *et al.* The 2010 European Venus Explorer (EVE) mission proposal. *Exp. Astron.* **33**, 305–335 (2012).
- Weidmann, D., Rose, R. & Jenkins, M. A fully integrated, miniaturized quantum cascade laser heterodyne radiometer for EO, presented at NCEO/CEOI Conference, Nottingham (2012).
- Moroño, A. & Hodgson, E. R. Radiation induced optical absorption and radioluminescence in electron irradiated SiO₂. *J. Nucl. Mater.* **258–263**, 1889–1892 (1998).
- Woody, C. L., Kierstead, J. A., Levy, P. W. & Stoll, S. Radiation damage in BaF₂ crystals. *IEEE Trans. Nucl. Sci.* **NS-39**, 515–523 (1992).
- El-Said, A. S. *et al.* Study of heavy-ion induced modifications in BaF₂ and LaF₃ single crystals. *Nucl. Instrum. Meth. B.* **218**, 492–497 (2004).
- Izerrouken, M., Meftah, A. & Nekka, M. Color centers in neutron-irradiated Y₃Al₅O₁₂, CaF₂ and LiF single crystals. *J. Lumin.* **127**, 696–702 (2007).
- Fernández-Rodríguez, M., Alvarado, C. G., Núñez, A. & Álvarez-Herrero, A. Analysis of optical properties behaviour of clearceram, fused silica and CaF₂ glasses exposed to simulated space conditions. In *International Conference on Space Optics* **4**, 8–13 (2010).
- Orlinski, D. V. & Gritsyna, V. T. Radiation resistance investigation of quartz glass KU-1. *Problems of Atomic Science and Technology*. No. 3. *Series: Plasma Physics* (5), 60–63 (2000).
- Kristianpoller, N., Rehavi, A., Shmilevich, A., Weiss, D. & Chen, R. Radiation effects in pure and doped Al₂O₃ crystals. *Nucl. Instrum. Meth. B.* **141**, 343–346 (1998).
- Islamov, A. Kh., Ibragimova, E. M. & Nuritdinov, I. Radiation-optical characteristics of quartz glass and sapphire. *J. Nucl. Mater.* **362**, 222–226 (2007).
- Izerrouken, M. & Benyahia, T. Absorption and photoluminescence study of Al₂O₃ single crystal irradiated with fast neutrons. *Nucl. Instrum. Meth. B.* **268**, 2987–2990 (2010).
- Zhang, M. F. *et al.* Effects of neutron irradiation and subsequent annealing on the optical characteristics of sapphire. *Physica B.* **406**, 494–497 (2011).
- Jie-cai, Han *et al.* Neutron irradiation and post annealing effect on sapphire by positron annihilation. *Appl. Radiat. Isotopes.* **68**, 1699–1702 (2010).

22. Plaksin, O. A. & Stepanov, V. A., Radiation-induced electrical and optical processes in materials based on Al₂O₃. *Opt. Spectrosc.* **90**, No. 4, 542–551 (2001).
23. Plaksin, O. A. *et al.* Radioluminescence of alumina during proton and heavy ion irradiation. *Nucl. Instrum. Meth. B.* **206**, 1083–1087 (2003).
24. Skuratov, V. A., Gun, Kim Jong, Stano, J. & Zagorski, D. L. *In situ* luminescence as monitor of radiation damage under swift heavy ion irradiation. *Nucl. Instrum. Meth. B.* **245**, 194–200 (2006).
25. Brovotto, B., Maxia, V. & Salis, M. On the radioluminescent emission of BaF₂. *Il Nuovo Cimento D* **18**, 1107–1110 (1996).
26. Yanagida, Takayuki, Fujimoto, Yutaka, Koshimizu, Masanori & Fukuda, Kentaro. Scintillation properties of CdF₂ crystal. *J. Lumin.* **157**, 293–296 (2015).
27. Dafinei, I. *et al.* Low temperature scintillation in ZnSe crystals. *IEEE Trans. Nucl. Sci.* **57** No. 3, 1470–1474 (2010).
28. Kužel, P. & Petzelt, J. Time-resolved terahertz transmission spectroscopy of dielectrics. *Ferroelectrics* **239**, 949–956 (2000).
29. Bolivar, P. H. *et al.* Measurement of the dielectric constant and loss tangent of high dielectric-constant materials at terahertz frequencies. *IEEE Trans. Microw. Theory Techn.* **51**, 1062–1066 (2003).
30. Thamizhmani, L., Azad, A. K., Dai, Jianming & Zhanga, W. Far-infrared optical and dielectric response of ZnS measured by terahertz time-domain spectroscopy. *Appl. Phys. Lett.* **86**, 131111-1–131111-3 (2005).
31. Naftaly, M. & Miles, R. E. Terahertz time-domain spectroscopy: A new tool for the study of glasses in the far infrared. *J. Non-Cryst. Solids.* **351**, 3341–3346 (2005).
32. Naftaly, M. & Miles, R. E. Terahertz time-domain spectroscopy of silicate glasses and the relationship to material properties. *J. Appl. Phys.* **102**, 043517-1–043517-2 (2007).
33. Seung, Beom Kang *et al.* Optical and dielectric properties of chalcogenide glasses at terahertz frequencies. *ETRI J.* **31**, 667–674 (2009).
34. Zalkovskij, M. *et al.* Ultrabroadband terahertz spectroscopy of chalcogenide glasses. *Appl. Phys. Lett.* **100**, 031901-1–031901-4 (2012).
35. Molina Contreras, J. R., Ionescu, A. & Dascalu, T. THz-time domain spectroscopy of (001) ZnSe. *AIP Conference Proceedings.* **1472**, 114–120 (2012).
36. Sanjuan, F. & Tocho, J. O. Optical properties of silicon, sapphire, silica and glass in the terahertz range. *OSA Technical Digest (online) (Optical Society of America, paper LT4C.1)*. (2012).
37. Sporea, D., Mihai, L., Sporea, A., Ighigeanu, D. & Negut, D. Optical and THz evaluation of components for gas sensing spectroscopy in hazardous environments, NATO ARW on THz Diagnostics of CBRN Effects and Detection of Explosives & CBRN, Izmir, November 3–6, 2015.
38. Sporea, D., Mihai, L., Sporea, A., Craciun, G. & Manaila, E. Electron beam irradiation of materials and components to be used in mid-IR spectroscopy, Proc. SPIE 9899, *Optical Sensing and Detection IV*, 989900 (April 29, 2016), doi: 10.1117/12.2230234; <http://dx.doi.org/10.1117/12.2230234>.
39. Sporea, D. *et al.* Mid-IR detectors testing for space missions, *13th International Conference on Mid-Infrared Optoelectronics: Materials and Devices*, Beijing, China, September 18–22, 2016.
40. Holbert, K. E. Radiation Effects Damage, “EEE 598—Radiation Effects” (2012).
41. Ermolina, I., Darkwah, J. & Smith, G. Characterisation of crystalline-amorphous blends of sucrose with terahertz-pulsed spectroscopy: the development of a prediction technique for estimating the degree of crystallinity with partial least squares regression, *AAPS PharmSciTech* **15**, 253–260 (2014).
42. Sibik, J., Löbmann, K., Rades, T. & Zeitler, J. A., Predicting crystallization of amorphous drugs with terahertz spectroscopy, *Molecular pharmaceutics* **12**, 3062–3068 (2015).
43. Zalkovskij, M., Lavrinenko, A., Malureanu, R. & Jepsen, P. U. Terahertz time-domain spectroscopy of chalcogenide glasses and devices for terahertz radiation manipulation Doctoral dissertation, Technical University of Denmark, Department of Photonics (2013).
44. Antsygin, V. D. *et al.* Optical properties of borate crystals in terahertz region. *Optics Communications* **309**, 333–337 (2013).
45. Fan, W. *et al.* Dielectric properties of coals in the low-terahertz frequency region, *Fuel*, **162**, 294–304 (2015).
46. Yanagida, T. *et al.* Growth, optical properties, and scintillation light yield of CaF₂: Ce crystals with different Ce concentration, *Japanese J. Appl. Phys.*, **49**, 032601-1–032601-5 (2010).
47. Luo, J. *et al.* Luminescence and scintillation properties of BaF₂-Ce transparent ceramic, *Optical Materials* **58**, 353–356 (2016).

Acknowledgements

The authors acknowledge the financial support of the Romanian Space Agency (ROSA) through the project “Evaluation of Components for Space Applications - ECSA”, contract 67/2013. Some of the equipments used in this research were purchased in the frame of the project “Center for Advanced Lasers Technologies (CETAL)”, contract 8PM/2010, financed by UEFISCDI.

Author Contributions

D.S. and A.S. conceived the study and prepared the manuscript; L.M. made the optical and THz measurements and processed the data; I.V. run the alpha particles irradiation, done the simulations and performed the dosimetry; all the authors discussed the results and the manuscript.

Additional Information

Supplementary information accompanies this paper at <http://www.nature.com/srep>

Competing financial interests: The authors declare no competing financial interests.

How to cite this article: Sporea, D. *et al.* Optical and THz investigations of mid-IR materials exposed to alpha particle irradiation. *Sci. Rep.* **7**, 40209; doi: 10.1038/srep40209 (2017).

Publisher's note: Springer Nature remains neutral with regard to jurisdictional claims in published maps and institutional affiliations.



This work is licensed under a Creative Commons Attribution 4.0 International License. The images or other third party material in this article are included in the article’s Creative Commons license, unless indicated otherwise in the credit line; if the material is not included under the Creative Commons license, users will need to obtain permission from the license holder to reproduce the material. To view a copy of this license, visit <http://creativecommons.org/licenses/by/4.0/>

© The Author(s) 2017